

Simulations of light scattering spectra of a nanoshell on plane interface based on the discrete sources method

Elena Eremina ^{a,*}, Yuri Eremin ^{b,1}, Thomas Wriedt ^{c,2}

^a *Universitaet Bremen, Badgasteiner Street 3, 28359 Bremen, Germany*

^b *Faculty of Applied Mathematics and Computer Science, Moscow State University, Lenin's Hills, 119992 Moscow, Russia*

^c *Institut für Werkstofftechnik, Badgasteiner Street 3, 28359 Bremen, Germany*

Received 9 March 2006; received in revised form 27 April 2006; accepted 13 June 2006

Abstract

The resonance properties of nanoshells are of great interest in nanosensing applications such as surface enhanced Raman scattering or biological sensing. In this paper the discrete sources method has been applied to analyze the spectrum of evanescent light scattering from a nanoshell particle deposited near a plane surface. Based on the rigorous theoretical model, which allows to take into account all features of the scattering problem as: medium with frequency dispersion, presence of the interface, the objective aperture and its location and core-shell asphericity, the scattering spectrum of nanoshells was calculated. The dependence of the local nanoshell spectral density behavior on its properties is discussed.

© 2006 Elsevier B.V. All rights reserved.

1. Introduction

Due to multiple practical applications, which use spectral light scattering by nanoshells, there is growing interest in simulation of their spectral resonance properties using a rigorous computer model. Nanoshells are a type of nanoparticles composed of a dielectric core coated with an ultra-thin silver or gold shell. They are of great interest in different scientific, medical and technological applications due to their scattering behavior and their ability to demonstrate a tunable plasmon resonance response in the visible and infrared range of spectra. It has been found that the resonance spectrum peak of nanoparticles depends on its properties (size, shape, shell thickness etc.) [1–4]. Varying these parameters enables to shift the plasmon resonance peak to a required frequency domain. Due to these abilities

nanoshells became of interest for wide variety of applications: environmental, Raman, chemical and biological sensing, surface-enhanced and near field scanning optical microscopy.

In most methods using nanoshells the colloidal suspension containing particles is deposited on a glass prism. The incident unpolarized light, which is coupled into the glass prism and hits the glass water interface with an angle slightly above the critical angle of total internal reflection. This generates an exponentially decaying evanescent field near the interface in the lower refractive index medium (water). A nanoshell in the vicinity of the surface transforms the evanescent field into a scattered field. The scattered light is collected by a detector objective lens. By measuring of resonance position important data of the ambient medium and its variation can be obtained. This principle is used e.g. for viruses and immunoglobulin detection [5]. Nowadays the sensitivity of detecting devices is so high that even a resonance shift of 1 nm can be detected.

Another side of nanoshells application and synthesis consist in a high sensitivity of its plasmon resonance to

* Corresponding author. Tel: +49 421 218 3583; fax: +49 421 218 5378.
E-mail addresses: eremina@iwt.uni-bremen.de (E. Eremina), eremin@cs.msu.su (Y. Eremin), thw@iwt.uni-bremen.de (T. Wriedt).

¹ Tel./fax: +7 095 939 1776

² Tel.: +49 421 218 3583; fax: +49 421 218 2507.

the properties of nanoshell itself. Even a slight deviation in particle properties can essentially shift the position of its plasmon resonance, which complicates data interpretation. That is why a detailed theoretical analysis of the scattering properties of nanoshells seems to be important for their synthesis [6,7].

The first attempts to model resonance properties of nanoparticles were based on discrete dipole approximation (DDA) [8], finite difference time domain (FDTD) [9] or Mie theory [1]. Unfortunately such approaches do not allow to account for particle-surface scattering interaction completely. Recently it has been shown that taking into account rigorous mathematical model including interface is very important for correct data interpretation [10]. In this paper we applied the Discrete Sources Method (DSM) [11] to simulate light scattering by a nanoshell. DSM enables to take into account the whole environment of the scattering problem including complete scattering interaction of a particle and interface, actual objective aperture and its deposition, core-shell asphericity etc. DSM has already been applied to the investigation of the scattering by solid noble nanoparticles on a plane surface [12]. In this paper DSM model is extended to nanoshell particle. The main objective of this paper is to present detailed investigation of the scattering behavior of nanoshells spectral resonance and optimal choice of the parameters, like diameter and shell thickness which enable a shift of the resonance into the “biological window” of tissue (wavelength range 700–1100 nm). Based on computer simulation analysis we consider the appropriate choice of nanoshell diameter, shell thickness and incident angle, which provide maximum response for the scattering field. Additionally the influence of the position of the objective lens is discussed.

The paper consists of four parts: in the first one the theoretical outlines of the DSM are given, the second part is devoted to the numerical scheme and in the final part of the paper we present simulation results and discussion.

2. Discrete sources method

In this section we would like to outline the DSM theory as presented in previous papers [11,12].

Consider an axial symmetric penetrable particle with interior domain D_i covered with a layer D_l and smooth external boundaries $\partial D_{i,l}$ deposited on the plane prism surface Σ . We denote the prism domain by D_1 and ambient space exterior to the nanoshell particle by D_0 . Let us introduce a Cartesian coordinate system $Oxyz$ by choosing its origin O at the interface surface and Oz coincides with the axis of symmetry of the particle and is directed into domain D_0 so, that plane $z = 0$ corresponds to the Σ plane. We assume that the exciting field $\{\mathbf{E}^0, \mathbf{H}^0\}$ is a plane wave propagating from D_1 at the angle θ_1 with respect to the z -axis (Fig. 1).

Then the mathematical statement of the scattering problem can be formulated in the following form:

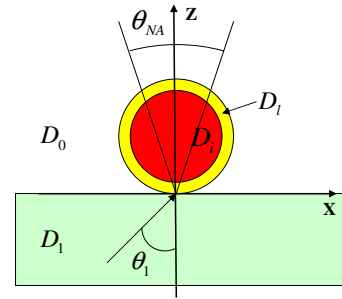


Fig. 1. Model geometry.

$$\begin{aligned} \nabla \times \mathbf{H}_\zeta &= jk\varepsilon_\zeta \mathbf{E}_\zeta; \quad \nabla \times \mathbf{E}_\zeta = -jk\mu_\zeta \mathbf{H}_\zeta \quad \text{in } D_\zeta, \zeta = 0, 1, i, l, \\ \mathbf{n}_i \times (\mathbf{E}_i - \mathbf{E}_l) &= 0, \quad \mathbf{n}_i \times (\mathbf{H}_i - \mathbf{H}_l) = 0, \quad \text{at } \partial D_i \\ \mathbf{n}_l \times (\mathbf{E}_l - \mathbf{E}_0) &= 0, \quad \mathbf{n}_l \times (\mathbf{H}_l - \mathbf{H}_0) = 0, \quad \text{at } \partial D_l \\ \mathbf{e}_z \times (\mathbf{E}_0 - \mathbf{E}_1) &= 0, \quad \mathbf{e}_z \times (\mathbf{H}_0 - \mathbf{H}_1) = 0, \quad \text{at } \Sigma \end{aligned} \quad (1)$$

and radiation conditions for the scattered field at infinity.

Here, $\mathbf{n}_{i,l}$ are the outward unit normal vectors to the surfaces, $k = \omega/c$ and $\{\mathbf{E}_\zeta, \mathbf{H}_\zeta\}$ stands for the total field in the corresponding domain $D_\zeta, \zeta = 0, 1, i, l$. Note that the total field in D_0 is a superposition of an exciting field and a scattered one. If $\text{Im}\varepsilon_\zeta, \mu_\zeta \leq 0$, the time dependence for the fields is chosen as $\exp\{j\omega t\}$ and the surfaces are smooth enough $\partial D_{i,l} \subset C^{(2,\alpha)}$, then the above boundary-value scattering problem is uniquely solvable [13].

We construct an approximate solution to the scattering problem (1) based on the DSM. First the plane wave $\{\mathbf{E}^0, \mathbf{H}^0\}$ scattering problem on the interface is solved. The result yields external excitation fields $\{\mathbf{E}_\zeta^0, \mathbf{H}_\zeta^0\}, \zeta = 0, 1$ in domains $D_{0,1}$, which satisfy transmission conditions at the plane interface. Let us construct the approximate solution of the boundary value problem (1) for the scattered field $\{\mathbf{E}_\zeta^s, \mathbf{H}_\zeta^s\}$ in $D_{0,1}$ and the total field in $D_{i,l}$.

In the frame of DSM the approximate solution is constructed by representing the electromagnetic fields as a finite linear combination of the electric and magnetic fields of multipoles distributed over an axis of symmetry inside the scatterer. Besides the fields analytically satisfy the transmission conditions enforced at the plane interface Σ [14], which provides an opportunity to account for whole interactions between scatterer and interface. Then the approximate solution satisfies the Maxwell equations in the domains $D_\zeta, \zeta = 0, 1, i, l$, the infinity conditions and the transmission conditions at the plane interface Σ . Thus, the scattering problem is reduced to the problem of approximation of the exciting field on the surfaces $\partial D_{i,l}$. Only the amplitudes of discrete sources (DS) are to be determined from the boundary conditions at the surfaces $\partial D_{i,l}$, which can be rewritten in following form:

$$\begin{aligned} \mathbf{n}_i \times (\mathbf{E}_i - \mathbf{E}_l) &= 0 \quad \mathbf{n}_i \times (\mathbf{H}_i - \mathbf{H}_l) = 0 \quad \text{at } \partial D_i \\ \mathbf{n}_l \times (\mathbf{E}_l - \mathbf{E}_0^s) &= \mathbf{n}_l \times \mathbf{E}_0^0 \quad \mathbf{n}_l \times (\mathbf{H}_l - \mathbf{H}_0^s) = \mathbf{n}_l \times \mathbf{H}_0^0 \quad \text{at } \partial D_l \end{aligned} \quad (2)$$

where $\{\mathbf{E}_0^0, \mathbf{H}_0^0\}$ is the refracted field into D_0 .

To generate the fields of multipoles, which analytically satisfy the transmission conditions at the plane interface Σ we should incorporate the Green's tensor of a half-space. The components of the Green's tensor accept the form of Sommerfeld integrals [12]. The approximate solution to the scattering problem is constructed taking into account the rotational symmetry of the scattering problem geometry (particle plus interface) and the polarization of the external excitation as well [11].

Consider P-polarized plane wave excitation. In this case the refracted plane wave into D_0 accepts the form

$$\mathbf{E}_0^0 = T^P(-\mathbf{e}_x \cos \theta_0 + \mathbf{e}_z \sin \theta_0)\chi_0, \quad \mathbf{H}_0^0 = -T^P n_0 \mathbf{e}_y \chi_0, \\ \chi_0 = \exp[-jk_0(x \sin \theta_0 + z \cos \theta_0)]. \quad (3)$$

Here $\eta_\xi = \sqrt{\varepsilon_\xi \mu_\xi}$ is associating refractive index of D_ξ , θ_0 is a refraction angle for the plane wave. The refraction coefficient $T_{1,0}^P$ can be written as $T_{1,0}^P = \frac{2n_1 \cos \theta_1}{n_1 \cos \theta_0 + n_0 \cos \theta_1}$. Snell's law in this case yields: $\sin \theta_0 = \frac{n_1}{n_0} \sin \theta_1$. As $|n_1| > |n_0|$ with increasing of incident angle θ_1 from 0 till $\pi/2$ one can get $|\sin \theta_0| > 1$. This circumstance requires corresponding branch for $\cos \beta_0 = -i\sqrt{\sin^2 \beta_0 - 1}$. Hence beyond the critical angle $\theta_c = \arcsin \frac{n_0}{n_1}$ in the upper half-space an evanescent wave appears, which is propagated along the interface and damping in the normal ($z > 0$) direction $\chi_0 = \exp\{-ik_0 x \sin \beta_0\} \exp\{-k_0 z \sqrt{\sin^2 \beta_0 - 1}\}$ [15].

Representations for the scattered field in D_0 and total field inside in D_i will be the same as in case of homogeneous particle considered in [12]. Let us focus on the representation of the total field inside the shell domain D_l . To adjust the polarization of exciting plane wave (3) we shall use following vector potentials:

$$\mathbf{A}_{mn}^{e,\kappa} = \{Y_m^\kappa(\zeta, z_n^\kappa) \cos(m+1)\varphi; -Y_m^\kappa(\zeta, z_n^\kappa) \sin(m+1)\varphi; 0\} \\ \mathbf{A}_{mn}^{h,\kappa} = \{Y_m^\kappa(\zeta, z_n^\kappa) \sin(m+1)\varphi; Y_m^\kappa(\zeta, z_n^\kappa) \cos(m+1)\varphi; 0\}; \\ \mathbf{A}_n^{e,\kappa} = \{0; 0; Y_0^\kappa(\zeta, z_n^\kappa)\}. \quad (4)$$

where $\kappa = l\pm$ and $Y_m^{l\pm}(q, z_n^{l\pm}) = \frac{k_0}{i} h_m^{(2)}(k_0 R_{\zeta z_n^{l\pm}})(k_0, \rho/R_{\zeta z_n^{l\pm}})^m$, $Y_m^{l-}(q, z_n^{l-}) = j_m(k_1 R_{q z_n^{l-}})(k_1, \rho/R_{q z_n^{l-}})^m$, $R_{\zeta z_n} = \rho^2 + (z - z_n)^2$. Here $j_m(\cdot)$ are the spherical Bessel functions, $h_m^{(2)}(\cdot)$ are the spherical Hankel functions, coordinates of multipoles $\{z_n^{l\pm}\} \in Oz$, and $\{z_n^{l\pm}\} \subset D_i$. So, the fields inside the layer are presented as superposition of outgoing ($l+$) and standing ($l-$) waves.

Using the notations for the differential forms $D_{1,2}^\zeta$ introduced in [12], we can construct our approximate solution as follows:

$$\begin{pmatrix} \mathbf{E}_\zeta^N \\ \mathbf{H}_\zeta^N \end{pmatrix} = \sum_{m=0}^M \sum_{n=1}^{N_m^\zeta} \{p_{mn}^\zeta D_1^\zeta \mathbf{A}_{mn}^{e,\zeta} + q_{mn}^\zeta D_2^\zeta \mathbf{A}_{mn}^{h,\zeta}\} + \sum_{n=1}^{N_0^\zeta} r_n^\zeta D_1^\zeta \mathbf{A}_n^{e,\zeta}, \\ \zeta = 0, i, l\pm, \quad (5)$$

$$\mathbf{E}_1^N = \mathbf{E}_{l+}^N + \mathbf{E}_{l-}^N; \mathbf{H}_1^N = \mathbf{H}_{l+}^N + \mathbf{H}_{l-}^N.$$

We would like to emphasise that the scattered field $\{\mathbf{E}_0^N, \mathbf{H}_0^N\}$ in domains $D_{0,1}$ can be represented in terms of the unitary set of amplitudes $\{p_{mn}^0, q_{mn}^0, r_n^0\}$. This circumstance

seems to be a key feature because it allows taking into account all the interactions between scatterer and interfacing analytically.

Similar approach can be implemented for S-polarized external excitation, see [12] for more details.

The completeness of the system of lowest-order distributed multipoles used in (5) guarantees convergence of the approximate solution to the exact one in any closed subset of D_0 [9].

3. Numerical scheme of the DSM

In this section a short description of the numerical scheme will be given. As mentioned above representation (5) satisfies all the conditions of the scattering problem (1) except the transmission conditions at the shell and core surfaces (2). These boundary conditions are used to determine the unknown amplitudes of DS $\{p_{nm}^{0,i,l\pm}, q_{nm}^{0,i,l\pm}, r_n^{0,i,l\pm}\}_{n=1}^{N_m^\zeta}$, $\zeta = 0, i, l$. Since the scattering problem geometry is axially symmetric with respect to the z -axis and the DS are distributed over the axis of symmetry, fulfilling the transmission conditions (2) at the surfaces $\partial D_{i,l}$ can be reduced to a sequential solution of the transmission problems for the Fourier harmonics of the fields. So, instead of matching the fields on the scattering surfaces $\partial D_{i,l}$ (see (2)), we can match their Fourier harmonics separately thus reducing the approximation problem on the surfaces to a set of problems enforced at the particle core and shell generatrices $\mathfrak{T}_{i,l}$. By solving these problems one can determine the DS amplitudes $\{p_{nm}^{0,i,\pm l}, q_{nm}^{0,i,\pm l}, r_n^{0,i,\pm l}\}_{n=1}^{N_m^\zeta}$.

We will use point-matching technique to fit the transmission conditions (2) for Fourier harmonics of the fields at the generatrices $\mathfrak{T}_{i,l}$. Let us consider matching points $L_{i,l}$ distributed over $\mathfrak{T}_{i,l}$ and corresponding number of multipoles for each domain: $N_m^0, N_m^i, N_m^{l\pm}$. In this case for each Fourier harmonic $m = 0, 1, \dots, K$ we get linear system for DS amplitudes of following dimension:

$$4(L_i + L_l) \times 2(N_m^0 + N_m^i + N_m^{l-} + N_m^{l+}).$$

It has been found that more stable results can be obtained by using the generalized point-matching technique and a pseudo-solution of an over-determined system of linear equations [14]. Because the DSM is a direct method and hence it allows to solve the scattering problem for the entire set of incident angles θ_1 and for both polarizations (P and S) at once. This is an advantage compared with methods similar DDA and FDTD. Besides, the numerical scheme provides an opportunity to control the actual convergence of the approximate solution to the exact one by a-posteriori error estimation [9].

Once the amplitudes of the DS were determined, one can calculate the far field pattern $\mathbf{F}(\theta, \varphi)$ of the scattered field, which is determined at the upper part of the unite semi-sphere $\Omega = \{0^\circ \leq \theta < 90^\circ, 0^\circ \leq \varphi \leq 360^\circ\}$ and is given by

$$\mathbf{E}(\mathbf{r})/|\mathbf{E}_0^0(0)| = \frac{\exp\{-ik_0 r\}}{r} \mathbf{F}(\theta, \varphi) + O(1/r^2), \quad r \rightarrow \infty$$

We asymptotically estimate the Sommerfeld integrals involved in the representation for the scattered field, which yields the representation for the θ, φ -components of the far field pattern $F_{\theta, \varphi}(\lambda, \theta, \varphi)$ as a finite linear combination of elementary functions, see [12] for more details. This circumstance ensures a low-costs computer simulations of the scattering characteristics in the far zone.

In the paper the intensity of scattered light is considered

$$I^{P,S}(\lambda, \theta, \varphi) = |F_{\theta}^{P,S}(\lambda, \theta, \varphi)|^2 + |F_{\varphi}^{P,S}(\lambda, \theta, \varphi)|^2$$

where $F_{\theta, \varphi}^{P,S}(\lambda, \theta, \varphi)$ are the components of the far field pattern for P and S polarized incident wave at the unit sphere θ, φ . The scattered intensity of an unpolarized wave calculated in $\mu\text{m}^2/\text{sr}$ units is also considered

$$I(\lambda, \theta, \varphi) = \frac{1}{2}(I^P(\lambda, \theta, \varphi) + I^S(\lambda, \theta, \varphi)) \quad (6)$$

We will also consider the detector objective scattering cross-section, which represents the summarized intensity scattered into the prescribed solid angle Ω

$$\sigma(\lambda) = \int_{\Omega} I(\lambda, \theta, \varphi) d\omega \quad (7)$$

where $\Omega = \{0 \leq \varphi \leq 360^\circ; 0 \leq \theta \leq 22.08^\circ\}$, which corresponds the Numerical Aperture of the objective lens $\text{NA} = 0.5$.

DSM provides the opportunity to control the accuracy of the computational result in two steps:

1. Control of the internal convergence of the results by increasing the number of matching points and DS;
2. Checking the residual in least square norm of the boundary conditions at the particle surface (2). As a rule a residual of 1% provides stabilization of the 2 digit of the scattering diagram.

In all the results presented below the residual was less then 0.2%.

The number of matching points where the DS amplitudes are defined increases until the necessary accuracy of the results is achieved. The DS number usually is 2–4 times less then the number of matching points. As a rule the DS are deposited on the axis of symmetry inside the particle. In the case of an oblate particle it is necessary to make an analytical continuation of the DS coordinates into the complex plane adjacent to the symmetry axis; DS then are deposited in the complex plane [11]. The maximal order of multipoles (K) is a priori defined from the condition that error of the plane wave approximation by corresponding Fourier series should be less then 0.1%. The detailed algorithm for matching point's choice is described in [14].

DSM model has been verified by comparison with Bobbert Vlioger model available in Th. Germer group at NIST [16] and with T-matrix code available in Th. Wriedt group at Bremen University [17].

4. Results and discussion

In this section we will present some numerical results obtained using the DSM model and discuss them shortly. As external excitation unpolarized light in the wavelength range of $400 \leq \lambda \leq 800 \text{ nm}$ has been taken. We investigated a nanoshell with PSL core and a thin shell of noble metal. As substrate material we took silica glass, the numerical aperture of objective $\text{NA} = 0.5$ has been used. For most of results presented here we took the fixed incident angle of 63° , which is close to the critical angle ($\sim 62^\circ$) corresponding to the whole wavelength range. In all the results the core diameter decreased with increase the shell thickness, but the external diameter of shell (D) stayed the same.

We would like to start with the investigation of the influence of shell thickness on the scattering response. For this propose we calculated the objective response for nanoshells of diameter $D = 50 \text{ nm}$ for different shell thicknesses and different shell material. The obtained results are shown in Figs. 2–4.

In Fig. 2 the results for PSL particle with gold (Au) shell are presented. From the results it is obvious that with decreasing of the shell thickness the peak of maximum

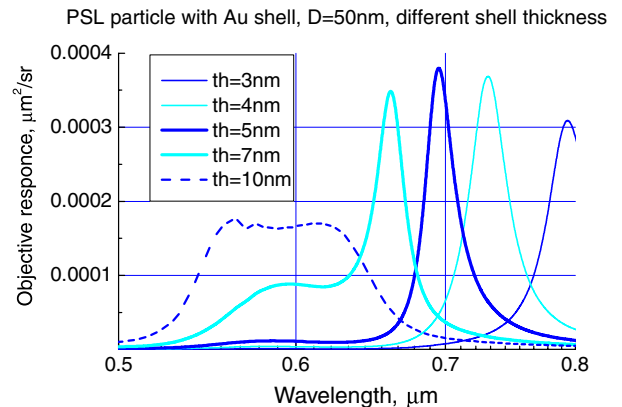


Fig. 2. Objective scattering response versus wavelength for Au nanoshell $D = 50 \text{ nm}$ with different shell thicknesses (th).

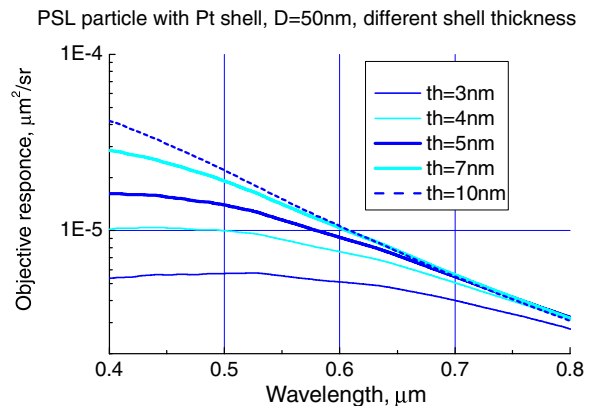


Fig. 3. Objective scattering response versus wavelength for Pt nanoshell $D = 50 \text{ nm}$ with different shell thicknesses.

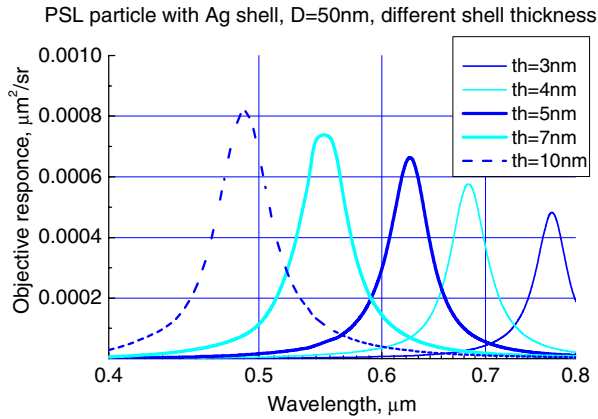


Fig. 4. Objective scattering response versus wavelength for Ag nanoshell $D = 50$ nm with different shell thicknesses.

shifts to the area of longer wavelength (red shift). The width of the peak also differs depending on the thickness of a shell. The results presented in Fig. 2 look similar to the experimental results presented in Fig. 1(b) in [1]. Similar results for platinum (Pt) and silver (Ag) shells are presented in Figs. 3 and 4. The results for silver shell look very close to those for the gold ones, but platinum nanoshell does not demonstrate any resonance peak in this range of spectrum under investigation. The objective response from a platinum nanoshell does not have a resonance peak and the curves smoothly decrease with increase of the incident wavelength for all shell thicknesses. Due to this fact we did not use platinum for further investigations and concentrated on silver and gold shells. The refractive index data for PSL can be found at Sematech website (see www.sematech.org), for noble particles and for substrate materials can be found in public sources [18,19] or in [20].

As we have already mentioned above that the objective of our research is not only to investigate the influence of different parameters of the scattering response, but also to find out the appropriate shell-core-diameter combination which provide a shift of the intensity peak to the area of biological window and also realise a sharp resonance peak. From analysis of the presented figures we found that a shell thickness of 3 nm would be the most reasonable choice for both gold and silver shells.

To find the appropriate particle diameter let us fix the shell thickness of 3 nm, and vary the diameter of the particle. In Fig. 5 results for the silver shell thickness of 3 nm are presented for various particle diameters. From these results one can see that with an increase of the diameter not only the intensity of the peak increases, but also the intensity maximum shifts to the area of longer wavelength and the peak gets wider. Similar results are presented for gold shell in Fig. 6. The optimal diameter which provides relatively high intensity and sharper peak corresponds to $D = 50$ nm. Let us now fix both the particle diameter and the shell thickness and turn to the choice of the incident angle we kept fixed up to now.

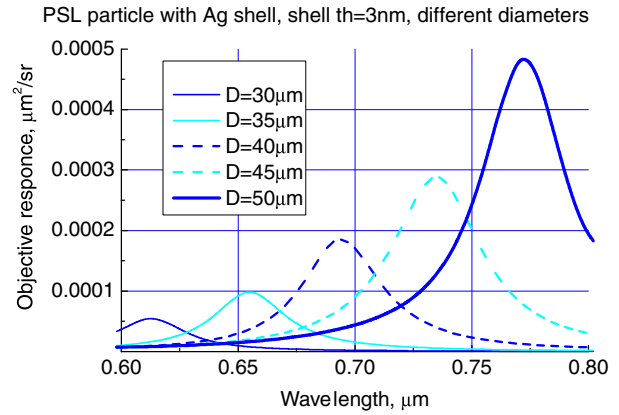


Fig. 5. Objective scattering response versus wavelength for Ag nanoshell with fixed shell thickness $th = 3$ nm and different diameters.

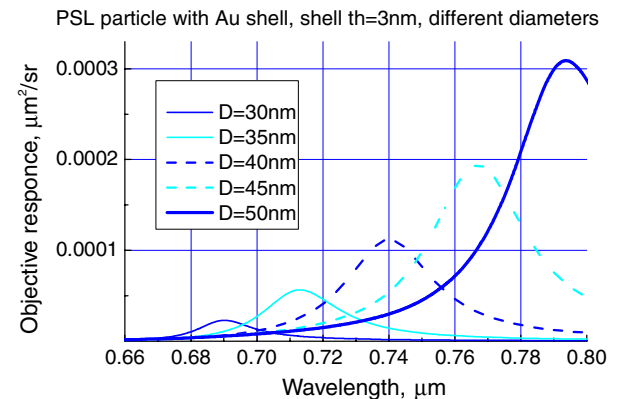


Fig. 6. Objective scattering response versus wavelength for Au nanoshell with fixed shell thickness $th = 3$ nm and different diameters.

In Fig. 7 the objective response for a silver shell for different incident angles is demonstrated. From the results one can see that the resonance wavelength stays the same, but its value decreases with the increasing of the incident angle. Consider the influence of objective lens shift with respect to the axis of symmetry on the response. Fig. 8 demonstrates the objective response for the silver nanoshell and for objective declinations of 15° and 40° from normal

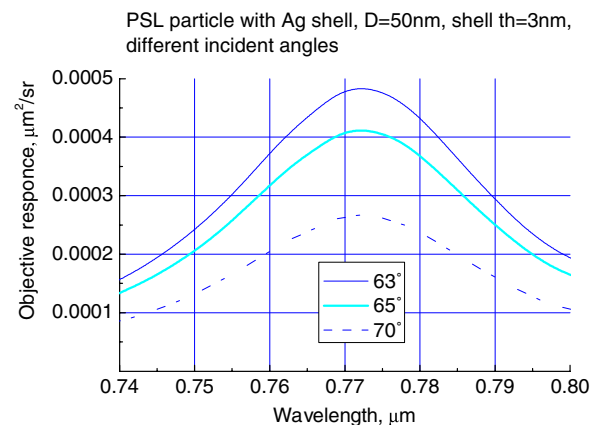


Fig. 7. Objective scattering response versus wavelength for Ag nanoshell of $D = 50$ nm with shell thickness of 3 nm for different incident angles.

PSL particle with Ag shell, $D=50\text{nm}$, shell thickness 3nm, inc. 63°
different objective deposition

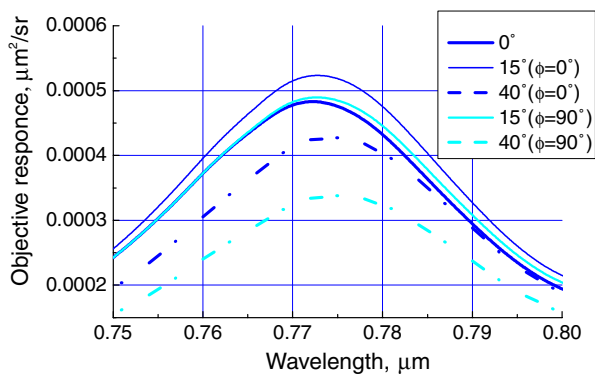


Fig. 8. Objective scattering response versus wavelength for Ag nanoshell of $D = 50\text{ nm}$ with shell thickness of 3 nm for different objective deposition.

direction to the interface in the incident plane ($\phi = 0$) and in the perpendicular direction ($\phi = 90$) under the incidence of 63° . From the results one can see, that highest response is found for a lens declination of 15° in the plane of incidence ($\phi = 0$).

Let us analyse another important aspect the nanoshell application – core-shell asymmetry. Nanoshell asymmetry, which does not often taken into account in theoretical consideration, appears rather often [21]. Fig. 9 shows the scattering response from silver nanoshell of $D = 50\text{ nm}$ with shell thickness of 3 nm under the incidence of 63° for various centre of the core deposition with respect to shell centre. The shift in this case means that the centre of core is shifted up (+) or down (–) inside nanoshell. From the simulation results one can see that even a small core-shift of 1 nm shifts the maximum of the response by about $10\text{--}15\text{ nm}$ and yields a decrease of its value. So, a possible asymmetry of the nanoshells should be taken into account in the design, as in sensitive systems the shift of resonance peak of even 10 nm could lead to the wrong interpretation of the measurements.

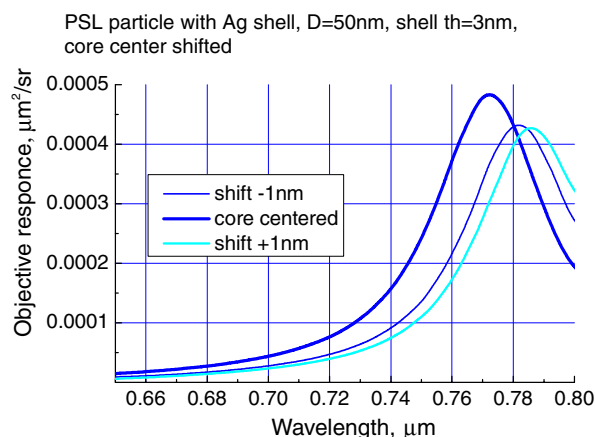


Fig. 9. Objective scattering response versus wavelength for Ag nanoshell of $D = 50\text{ nm}$ with shell thickness of 3 nm for different asymmetry models.

5. Conclusion

In this paper DSM has been applied to analyze scattering behaviour of nanoshells on a glass prism. The main objective of research was to investigate the influence such parameters as: nanoshell diameter, shell thickness, angle of incidence and position of the objective lens on the scattering response. The results obtained by simulation using DSM model allow to choose the optimal parameters for nanoshells, which provide shift of the resonance peak into the window of biological transparency: $D = 50\text{ nm}$, shell thickness of about 3 nm and incident angle close to the critical angle. We can also as conclude that measuring set up seems to be less sensitive to the choice incident angle and objective lens location, because of variations examined keep the same spectral peak position. It has also been demonstrated that the scattering behaviour strongly depends on the core-shell asymmetry, which may lead to incorrect interpretation of experimental results.

Acknowledgements

We gratefully acknowledge funding of this research by Deutsche Forschungsgemeinschaft (DFG) and the Russian Foundation for Basic Research (RFBR).

References

- [1] G. Raschke et al., Nanoletters 4 (10) (2004) 853.
- [2] J.J. Mock, D.R. Smith, S. Schultz, Nanoletters 3 (4) (2003) 485.
- [3] R.D. Averitt, D. Sarkar, N.J. Halas, Phys. Rev. Lett. 78 (22) (1997) 4217.
- [4] D.D. Evanoff Jr., G. Chumanov, J. Phys. Chem B 108 (2004) 13957.
- [5] L.R. Hirsch, J.B. Jackson, A. Lee, N.J. Halas, J.L. West, Anal. Chem. 75 (2003) 2377.
- [6] L. Ren, G.M. Chow, Mater. Sci. Eng. C23 (2003) 113.
- [7] H.S. Zhou, I. Honna, H. Komiyama, Phys. Rev. B 50 (16) (1994) 12052.
- [8] K. Kelly, E. Coronado, Lin Zhao, G. Schatz, J. Phys. Chem. B 107 (2003) 668.
- [9] J.B. Jackson, N.J. Hallas, PNAS Proc. 101 (52) (2004).
- [10] N. Grishina, Yu. Eremin, Opt. Spectro. 97 (5) (2004) 803.
- [11] Yu. Eremin, J. Commun. Technol. Electron. 45 (2) (2000) 269.
- [12] E. Eremina, Y. Eremin, T. Wriedt, Opt. Commun. 246 (2005) 405.
- [13] D. Colton, R. Kress, Inverse Acoustic and Electromagnetic Scattering Theory, Springer, Berlin, 1992.
- [14] Y. Eremin, N. Orlov, A. Sveshnikov, in: T. Wriedt (Ed.), Generalized Multipole Techniques for Electromagnetic and Light Scattering, Elsevier Science, Amsterdam, 1999, p. 39.
- [15] J.A. Kong, Electromagnetic Wave Theory, EMW Publ., Cambridge, MA, 2000.
- [16] <http://physics.nist.gov/Divisions/Div844/staff/Gp6/germer.html>.
- [17] A. Doicu, T. Wriedt and Y. Eremin, Null-Field Method with Discrete Sources – Theory and Programs, Springer, Berlin, Heidelberg, New York, in press.
- [18] http://www.mellesgriot.com/products/optics/mp_3_1.htm.
- [19] Michael Thomas Flanagan's Java Library Refractive Index Class: <http://www.ee.ucl.ac.uk/~mflanaga/java/RefractiveIndex.html>.
- [20] P. B Johnson, R.W. Christy, Phys. Rev. B 6 (12) (1972) 4370.
- [21] J.-E. Jönsson, O.J. Karlsson, H. Hassander, B. Törnell, Macromolecules 34 (2001) 1512.